# Small in-stream barriers contribute little to strong local population genetic structure in five hololimnic macroinvertebrate taxa

Martina Weiss[1,2]*, Hannah Weigand[1,3], Florian Leese[1,2]

[1] Aquatic Ecosystem Research, University of Duisburg-Essen 45141 Essen, Germany

[2] Centre for Water and Environmental Research (ZWU), University of Duisburg-Essen 45141 Essen, Germany

[3] Musée National d'Histoire Naturelle, 2160 Luxembourg, Luxembourg

**Keywords:** gene flow – *Gammarus* – *Ancylus* – *Dugesia* – genomics

*Corresponding author: Martina Weiss, Aquatic Ecosystem Research, University of Duisburg-Essen 45141 Essen, Germany, Fax: 0049-201-183-3990, E-mail: martina.weiss@uni-due.de

**Abstract**

**1.** River networks are frequently fragmented by in-stream barriers. These man-made obstacles can act as dispersal barriers for aquatic organisms and can isolate populations, thereby increasing the effects of genetic drift and inbreeding, and leading to the loss of genetic diversity. Although millions of small in-stream barriers exist worldwide, such as ramps, drops below 2 m, tunnels and pipes, their impact on dispersal of ecologically important, hololimnic macroinvertebrate taxa is unclear. We assessed the effects of such barriers on the population structure and effective dispersal of five hololimnic macroinvertebrate taxa with different dispersal capacities.

**2.** We studied populations of the amphipod *Gammarus fossarum* (clade 11), three snail species of the *Ancylus fluviatilis* species complex and the planarian *Dugesia gonocephala*, at 15 barrier sites in the heavily fragmented catchment of the river Ruhr (Germany). Nine weirs and eight culverts with ages of 33–109 years were investigated. Genome-wide SNP data were obtained via double digest restriction-site associated DNA sequencing (ddRAD). To assess fragmentation and barrier effects, we evaluated clustering, differentiation between populations up- and downstream of each barrier, and effective migration rates among sites and across barriers. Additionally, we used population genomic simulations to assess expected differentiation patterns under different gene flow scenarios.

**3.** Genomic data revealed that populations of all species were highly isolated at regional and local scales, suggesting that barriers substantially impede gene flow. Coupled with population genomic simulations, our data suggest that the analysed individual in-stream barriers are unlikely to be the cause of population fragmentation, although we found an effect of pipes (*A. fluviatilis* II and III) and some large ramps (>1.3 m; *D. gonocephala*).

**4.** Our comparative population genomic analysis shows that the actual population structure deviated from initial expectations for the five macroinvertebrate species, and that individual small in-stream barriers do not contribute substantially to the strong population differentiation.

**5.** The combination of highly resolving genomic markers, population genetic simulations and a controlled sampling design with distinct reference populations is a suitable approach to identify drivers of regional and local population structure.

## Introduction

Rivers in the Anthropocene are in crisis due to various human activities (Jackson et al., 2001; Vörösmarty et al., 2010). In particular, natural water flow has been altered substantially over the past few centuries by the construction of in-stream barriers, such as dams, weirs (Grill et al., 2015; Nilsson, Reidy, Dynesius, & Revenga, 2005; Zarfl, Lumsdon, Berlekamp, Tydecks, & Tockner, 2015) and culverts (David, Tonkin, Taipeti, & Hokianga, 2014; Torterotot, Perrier, Bergeron, & Bernatchez, 2014; Wheeler, Angermeier, & Rosenberger, 2005). Such human-induced habitat fragmentation is considered a major threat to biodiversity (Hudman & Gido, 2013). In isolated populations, the effects of genetic drift and inbreeding are higher, thereby increasing the risk of genetic diversity loss (e.g., Vrijenhoek, 1998) and extinction (Bijlsma & Loeschcke, 2012). To predict population resilience and long-term adaptability, it is therefore crucial to understand species-specific dispersal patterns (Hughes, Schmidt, McLean, & Wheatley, 2008) and to identify dispersal barriers.

In-stream barriers can impede in particular upstream dispersal, and influence the genetic structure of fragmented populations in fish (e.g., Hansen et al., 2014; Horreo et al., 2011; Junker et al., 2012; Torterotot et al., 2014; Van Leeuwen et al., 2018). However, few studies have focused on the effect of in-stream barriers on freshwater invertebrate taxa. Although barrier effects have been reported (David et al., 2014; Dillon, 1988; Resh, 2005), they are highly species-specific (Tonkin, Stoll, Sundermann, & Haase, 2014) owing to divergence in life history traits. Furthermore, little is known about the effects of smaller weirs and culverts, which fragment river systems and can occur at high densities, with less than 1 km between barriers (Dumont, Anderer, & Schwevers, 2005). There is often limited information about the properties of these small barriers, including the age of the barrier, shape, impoundment areas or velocity changes, making it difficult to predict their impact on genetic structure. Further, studying the effects of small in-stream barriers, which might impede dispersal only, or stronger in upstream direction, is especially challenging in macroinvertebrates with large effective population sizes and low dispersal ability (e.g., in hololimnic taxa). However, low effective dispersal alone can generate genetic background structure, which needs to be accounted for when studying impacts of in-stream barriers on genetic structure (Coleman et al., 2018). In addition to temporal

sampling or space-for-time study designs to distinguish between background genetic structure and barrier effects (Coleman et al., 2018), population genetic simulations can improve the interpretation of empirical data by generating null models under specific assumptions (e.g., life history traits) (Hoban, Bertorelle, & Gaggiotti, 2012). Considering the relatively young age of man-made barriers (typically tens of years to a few hundred years) and potential large population sizes of macroinvertebrate species, high-resolution markers, like genome-wide single nucleotide polymorphisms (SNPs), are needed to resolve fine-scale patterns of genetic structure (Whiterod, Zukowski, Asmus, Gilligan, & Miller, 2017).

The aim of this study was to evaluate the impact of small in-stream barriers on population genetic structure in various ecologically important hololimnic macroinvertebrates in a heavily anthropogenically impacted stream network. High-resolution genome-wide SNP data were generated by ddRAD sequencing (Peterson, Weber, Kay, Fisher, & Hoekstra, 2012). To account for species-specific genetic background structure, reference sites were sampled in each stream. Further, the distances between sites were chosen within the dispersal ability of all species (~200 m), so that without a barrier, gene flow should be high. All species, including the amphipod *Gammarus fossarum* clade 11 (after Weiss, Macher, Seefeldt, & Leese, 2014), the planarian *Dugesia gonocephala* and three snail species of the *Ancylus fluviatilis* species complex (*A. fluviatilis* I, II, III; Weiss, Weigand, Weigand, & Leese, 2018), are strictly confined to the aquatic environment (i.e., all are hololimnic) and commonly occur in rhithral streams in Europe but differ in feeding type, reproductive strategy and dispersal mode (Baršiene, Tapia, & Barsyte, 1996; Brittain & Eikeland, 1988; Burch, 1962; de Vries, 1986; Eder et al., 1995; Elliott, 2003; MacNeil, Dick, & Elwood, 1997; Minshall & Winger, 1968; Moog, 1995; Nesemann & Reischütz, 1995; Patrick, Cooper, & Uzarski, 2014; Schmidt-Kloiber & Hering, 2015).

Microsatellite and COI analyses have suggested that *G. fossarum* clade 11 and 12 are capable of overcoming in-stream barriers (Alp, Keller, Westram, & Robinson, 2012; Weiss & Leese, 2016). However, it is possible that barrier effects were concealed by confounding factors or that the marker resolution was too low. For the other species, no such information exists. In addition to using genome-

wide SNP data, we conducted population genetic simulations to test how species-specific life history traits influence the detectability of barrier effects. Based on mobility and population size, we hypothesised that the effect of in-stream barriers is weakest for *G. fossarum*, moderate for *D. gonocephala* and strongest for *A. fluviatilis* I, II and III (Figure 1). Further, for all taxa, we hypothesised that the effect of weirs depends on barrier properties, with the highest, steepest and smoothest barriers having the strongest effect. For culverts, we hypothesised that pipes have stronger effects than tunnels and that the effect depends on the length, diameter and sediment of the culvert, with longer culverts with a smaller diameter and concrete ground (instead of natural sediment) having the strongest effect.

## Materials and Methods

### Study design and study sites

The study region was the river Ruhr catchment (North Rhine-Westphalia, Germany), with many weirs and culverts, often separated by less than 1 km (Dumont et al., 2005). Taxa sampled were *G. fossarum* clade 11, *D. gonocephala* and *A. fluviatilis.* The three species *A. fluviatilis* I, II and III can only be identified by ddRAD analyses (Weiss et al., 2018); accordingly, specimens were sampled and processed in the lab as a single species. The sampling scheme was designed to systematically test the impact of two types of in-stream barriers, weirs (abbreviated QB) and culverts (VR), on gene flow. To compare gene flow among populations with and without a barrier in the same stream, specimens were sampled from at least three sampling sites (S), so that two sites were sampled upstream (S1 & S2) or downstream (S3 & S4) of the barrier with no barrier in-between. If possible, reference sites were sampled up- and downstream of the barrier. In one case (VR17), three reference sites were sampled upstream of the barrier. If tributaries joined the stream within the sampling range, specimens were collected at these locations (abbreviated N). In two cases, the scheme was extended to contain five sites (S0–S4) with a barrier downstream of S1 and S2 (VR6 and QB27). Based on the dispersal range of all target taxa, 200 m was chosen as the distance between sampling sites, including sites separated by a barrier. Specimens were collected at 15 barrier sites consisting of 17 barriers (Figure 2), including

eight culverts (8–120 m in length) and nine weirs (0.6–1.65 m in height) (Table 1). At single sampling sites, 5–12 specimens per species were sampled, but not all target species occurred at all sites.

**Genotyping**

DNA was extracted from muscle tissue using a salt-extraction protocol as described in Weiss and Leese (2016) for 344 *D. gonocephala* and 123 *A. fluviatilis* specimens. For *G. fossarum*, DNA from 315 specimens from a previous study (Weiss & Leese, 2016) was used. Four ddRAD libraries were generated for *D. gonocephala* (containing 83, 83, 87 and 89 samples), two for *A. fluviatilis* (62 and 61 samples) and four for *G. fossarum* ( 92, 66, 65 and 95 (3 repeated from library 1) samples) according to the protocol described in Vendrami et al. (2017), with modifications described in Weiss et al. (2018) and Weigand et al. (2018). An overview of the protocol with species-specific details and the general workflow is given in Appendix S1 and sample preparation details are given in Table S1. All samples for each library were pooled with equimolar concentrations and sequenced on an Illumina HiSeq 2500 sequencer to obtain 125 bp paired-end reads (Eurofins Genomics Europe Sequencing GmbH; Constance, Germany). For *A. fluviatilis*, data for three ddRAD libraries (269 specimens, Weiss et al., 2018) were also used, resulting in 389 specimens.

**ddRAD data analysis**

Pre-processing of ddRAD data for each sequencing library was conducted as described in Weiss et al. (2018). After pre-processing, denovo_map.pl of Stacks v.1.34 (Catchen, Hohenlohe, Bassham, Amores, & Cresko, 2013) was used to identify loci and genotypes. Stacks was run with eight different settings per species to identify the optimal parameter settings (Paris, Stevens, & Catchen, 2017, see Appendix S1 for details). Stacks results were exported from stacks databases with export_sql.pl (minimum stack depth 8). For *D. gonocephala*, aneuploid cytotypes are known besides diploids, with chromosome numbers similar to triploids (de Vries, 1986). Therefore, individual ploidy levels based on the expected allelic coverage was estimated using the R-script ploidyCounter.R (Rozenberg, https://github.com/evoeco/radtools/, see Weigand et al. 2018 for details).

Further analyses were performed using Snakemake workflows (Köster & Rahmann, 2012), combining stacks2fasta.pl (Macher et al., 2015) and several in-house python and R-Scripts for data reformatting, filtering and population genetic analyses. Parameter settings were similar for each species, except for *Ancylus* species, where parameters were adjusted when possible to account for polyploid genomes. First, Stacks parameter and locus filtering settings were optimised, as described in detail in Appendix S1. General population structure was analysed with individuals divided into populations according to barrier sites. The following locus filtering settings were chosen: 1–12 SNPs/locus (only one used), minor allele frequency 1%, locus present in at least 80% of individuals per population and 95% of all individuals. Further, specimens with too few reads or more than 20% missing data were excluded. Basic population genetic statistics were calculated using the R-package hierfstat (Goudet, 2005) in R v. 3.3.2 (R Core Team, 2015). Further, principal component analyses (PCAs; Patterson, Price, & Reich, 2006) were performed and individual ancestry coefficients were estimated based on sparse nonnegative matrix factorisation algorithms (sNMF; Frichot, Mathieu, Trouillon, Bouchard, & François, 2014) using the R-package LEA (Frichot & François, 2015) to identify genetic clusters. Both methods are suitable for polyploid and mixed ploidy data as they do not assume Hardy–Weinberg equilibrium (Dufresne, Stift, Vergilino, & Mable, 2014; Frichot et al., 2014). For sNMF analyses, number of clusters tested were k = 1–15 for *Ancylus* species and k = 1–17 for *G. fossarum* and *D. gonocephala*, and analyses were run with 30 replicates and 100,000 iterations per replicate. In addition, Neighbor-Net networks (Bryant & Moulton, 2004) were calculated using SplitsTree v. 4.14.5 (Huson & Bryant, 2006). Pairwise $F_{ST}$ values (after Weir & Cockerham, 1984) between barrier sites were calculated and significance was tested by bootstrapping over loci (10,000 replicates; 0.025/0.975 confidence intervals (CIs)) using the R-package hierfstat. $H_O$ and allelic richness (AR) in each population were calculated using the R-package diveRsity (Keenan, McGinnity, Cross, Crozier, & Prodöhl, 2013). Further, the divMigrate function (Sundqvist, Keenan, Zackrisson, Prodöhl, & Kleinhans, 2016) in this R-package was used to assess directional relative migration rates and to detect asymmetries in gene flow using Nei's $G_{ST}$ (Nei, 1973). To evaluate correlations of genetic distances with geographic distances (isolation by distance, IBD), Mantel tests were conducted

using the R-package vegan (Oksanen et al., 2019). As a measure of genetic distance, pairwise $F_{ST}$ values were calculated between all single sampling sites (S). For geographic distances, either straight-line or waterway distances were used. Both distances were calculated using QGIS v. 2.14.14 (http://qgis.org) with the same stream map used for the visualisation of sampling sites and population structure, provided by the federal state authority LANUV (Gewässerstationierungskarte des Landes NRW © LANUV NRW (2013)).

Finally, the effects of different in-stream barriers on gene flow among populations up- and downstream of barriers were analysed. To enable detection of low differentiation among adjacent sites, loci were exported separately for each barrier site with the same filter settings used for previous analyses, except the minor allele frequency was set to 5% and loci had to be present in 90% of specimens to account for the smaller sample sizes. For barrier analyses, two population definitions were used: population = sampling site (S) and population = S upstream/S downstream. $H_O$ and AR per population and pairwise $F_{ST}$ were calculated. The number of private alleles in each population was calculated using an in-house python script. To account for differences in population size, larger populations were randomly subsampled 30 times to match the smallest population size and the mean number of private alleles among replicates was calculated. DivMigrate was used to calculate migration rates between sampling sites and to assess asymmetric migration patterns. A large number of loci can partly compensate for the low sample sizes; however, results for populations with $n < 5$ should be interpreted with caution.

**Population genetic simulations**

To generate null models for population differentiation caused by migration barriers over time, Nemo 2.3.51 (Guillaume & Rougemont, 2006) was used. Within simulations, various barrier strengths and biological species traits were applied, including various mating systems (random mating for *G. fossarum* and hermaphrodite for *A. fluviatilis* and *D. gonocephala*), population sizes, extinction rates, selfing rates for hermaphrodites, and dispersal and barrier models (Appendix S1 and S2). The dispersal and barrier models were designed to reflect stream dispersal (linear, influenced by flow

direction) and our sampling scheme (four equidistant sampling sites). To prevent edge effects (no further dispersal possible for edge populations in the simulation), we simulated six populations but only analysed the four target populations. Simulations were run for 250 generations. The first 100 generations were simulated with different dispersal models but without a barrier to separate dispersal model and barrier effects. After 100 generations, a barrier was introduced for the next 150 generations using three models (complete barrier, upstream barrier with unchanged or reduced downstream dispersal), and fstat files were saved every five generations.

Data analyses were conducted using different python and R-Scripts in a Snakemake workflow. Edge populations were excluded, and ten individuals per population were randomly chosen. Populations with fewer than ten individuals at specific time points were excluded. Pairwise $F_{ST}$, $H_O$ and AR were calculated for all populations every five generations for each parameter combination, as described for ddRAD data. $F_{ST}$ values were calculated for all single populations and for pooled populations on both sides of the barrier. To evaluate the performance of divMigrate in the detection of reductions of migration rates due to barriers, a subset of output files generated with the migration model "asymmetric15" and all barrier models (except upstream barrier with reduced downstream 5%) was selected for random mating and hermaphroditic species for population sizes of 100 (500 for reduced downstream dispersal models) and 1000 with extinction rates of 0 or 0.6, and migration rates (using $G_{ST}$) were calculated at different time points before (5, 50 and 95 generations) and after barrier introduction (after 110, 150, 200 and 250 generations).

## Results

### Population structure of *Gammarus fossarum*

We found *G. fossarum* in nine streams at 11 barrier sites (see Table S2 for sampling size per site and Tables S3 and S4 for summary statistics for all species). PCA (Figure S1) and sNMF analyses indicated strong population structure. In the sNMF analysis, cross-entropy (CE) was lowest for k = 9 (Figure S2A). The nine clusters corresponded to the nine streams (Figure 3A). QB17&QB23 and VR6&VR17 were located in one stream each and clustered together by stream origin. In the Neighbor-

Net analysis, the same group structure was detected (Figure 3B). Further, the network showed superordinate clustering into three phylogenetically distinct groups in concordance with the sampling site topography. Populations from adjacent sites grouped together in the network, especially when considering stream network connectivity. The first cluster contained specimens from sites VR11, VR23 and VR12; the second included specimens from QB27, QB24 and QB17&QB23; and the third included individuals from QB12 and VR6&VR17, with QB22 intermediate between the last two clusters. Within the VR6&VR17 cluster, further sub-structure was detected. Pairwise $F_{ST}$ values were generally high (mean 0.47), especially between network-groups, and all values were significant, including values for the comparison between barrier sites in one stream, ranging between 0.01 and 0.74 (Figure S3A). Likewise, estimated migration rates were very low in most cases (mean 0.05), with the exception of within-stream comparisons (Figure 3D, Table S5A). However, migration rates between VR6&VR17 were much lower in both directions than those between QB17&QB23 (>0.89 in both directions), and were significantly higher in the downstream than in the upstream direction (VR6 to VR17: 0.29; VR17 to VR6: 0.13). In 71% of comparisons, significant asymmetric gene flow was detected.

**Population structure of *Dugesia gonocephala***

*D. gonocephala* was sampled at 13 barrier sites in 11 streams. Of 344 specimens, 294 were diploid and 50 were potentially triploid. PCA (Figure S1) and sNMF cluster analysis both indicated strong population sub-structuring. CE was lowest for K = 13 (Figure S2B). The group structure could be explained best by the stream and ploidy level (Figure 4A). At sites with both diploids and triploids (QB24, QB17&QB23 and VR9), individuals were divided into two clusters or showed high intermixture between clusters. At VR9, most “triploids” had a high membership to the stream-specific cluster. By contrast, diploid specimens only had a membership rate of 0.3–0.4% to VR9 and otherwise showed relatively high membership probabilities to many clusters. In QB22 (only diploids), specimens had the highest membership probabilities to their stream-specific clusters but also showed high membership to other clusters, especially specimens from the side stream (N).

The Neighbor-Net showed a star-like pattern containing 11 clusters, each representing a single stream (Figure 4B). The QB17&QB23 cluster contained two sub-clusters corresponding to the ploidy level. Similar results were obtained for QB24 and VR9; however, distances were lower. The VR6&VR17 cluster included two groups corresponding to barrier sites, but the distance was low. $F_{ST}$ values were lower than those for *G. fossarum* (mean: 0.31, range 0.08 to 0.51) but significant for all pairwise comparisons (Figure S3B). This applied to barrier sites within the same stream, but $F_{ST}$ values were low. In general, estimated migration rates were higher than those for *G. fossarum* (mean: 0.16) and migration rates for most comparisons were significantly asymmetric (73%; Figure 4D, Table S5B). Similar to *G. fossarum*, migration rates were highest between sites within a stream. In both streams, migration was significantly higher in the downstream direction than in the upstream direction (VR6 to 17: 0.88; VR17 to 6: 0.46; QB23 to 17: 1; QB17 to 23: 0.56). Further interconnected populations were found at sites QB20, QB22, VR9, VR11 and VR23, with the highest migration rates between VR9 and QB22. Of these, only populations at QB20 and QB22 were located in close proximity.

**Population structure of *Ancylus fluviatilis* I, II and III**

Among 389 specimens, 167 were assigned to *A. fluviatilis* I, 159 to *A. fluviatilis* II and 63 to *A. fluviatilis* III. In contrast to *G. fossarum* and *D. gonocephala*, $H_O$, $F_{ST}$ and $F_{IS}$ values varied strongly between stacks settings (Table S4). For *A. fluviatilis* I, PCA (Figure S1) and sNMF indicated strong genetic structure. CE values were low for cluster counts of 7 to 10 (Figure S2C), with the lowest mean CE over repetitions for k = 8. The clusters mainly corresponded to streams (Figure 5A). In QB27, two clusters were detected, present at all single sampling sites. At QB17, only one *A. fluviatilis* I specimen was found, which showed well-supported membership to the QB22 and QB12 & QB20 (one stream) clusters. High admixture was also found in some specimens from the VR9 cluster and the QB12 & QB20 cluster.

These results corresponded well with the network results (Figure 5B), where a similar group structure consistent with streams was visible, with the exception of specimens from QB12 and QB20,

which were split into two groups according to the barrier site. QB22 specimens clustered closely with those two groups, consistent with the relatively short geographic distance between sites, while all other sites (some separated by similar geographic distances) were separated by longer branches in the network. In general, pairwise $F_{ST}$ values were lower than those in *G. fossarum* and *D. gonocephala* (mean: 0.18, range: 0 – 0.29). However, for most comparisons, there was significant differentiation, with the exception of the within-stream comparison for specimens from QB11 & VR20 (Figure S3C). In general, migration rates were higher than those for *G. fossarum* but lower than those for *D. gonocephala* (mean: 0.11), with 80% of comparisons showing significant asymmetry (Figure 5D, Table S5C). Migration rates were highest between VR20 & QB11 (distance ~200 m) located in the same stream (0.86/1). For the other within-stream comparisons (QB12 & QB20, distance ~10 km), rates were much lower (0.19/0.22).

For *A. fluviatilis* II, PCA (Figure S1) and sNMF both indicated strong population structure within the species. The most probable number of clusters in the sNMF analysis was k = 8 (Figure S2D). The clusters were less clear than those for the other species, as many specimens showed high amounts of shared ancestry to different clusters. The main factor explaining the groups was stream origin (Figure 6A), but in some cases, main cluster were shared among different streams or additional cluster were found within one stream. A similar structure was observed in the Neighbor-Net analysis; however, single specimens, showing high admixture in the sNMF plot, grouped together with specimens sampled in other streams (Figure 6B). Overall, pairwise $F_{ST}$ values indicated relatively low but significant differentiation between all sampling sites, except for QB23–QB24 (mean: 0.08, range: 0.003 – 0.15). Estimated migration rates were higher than those for the other species (mean: 0.17) and less asymmetry was detected (58% of comparisons, Table S5D). Migration rates, at least in one direction, were highest between sites sampled within one stream (VR20/QB11: 0.47/1; QB23/QB17: 0.5/0.59) and between QB24 and QB23 (0.81/0.4), but were not high for QB24 and QB17 (0.22/0.15), even though this site was located between the other two (Figure 6D). However, at QB24, the sample size was low (n = 5).

*A. fluviatilis* III was mainly found in one stream with two barrier sites (VR6&VR17). At VR9, four individuals were identified as *A. fluviatilis* III/I hybrids (75%/25%) by Weiss et al. (2018), and these were included in the population genetic analysis of this species. In the PCA (Figure S1) and sNMF analysis, further population structure was detected, with four clusters best explaining the population structure (Figure S2E). One cluster consisted of VR9 specimens, the second of VR17 specimens and the other two of VR6 specimens, with shared proportions for some individuals in the VR6 and VR17 clusters (Figure 7A). A similar pattern was observed in the Neighbor-Net analysis (Figure 7B). Pairwise $F_{ST}$ values were all significant, but were lower between VR6 and VR17 (0.07) than between both sites and VR9 (0.3 and 0.27, respectively). Accordingly, migration rates were high between VR6 and VR17 (0.86/1), and low between VR9 and other sites (Figure 7D, Table S5E). Migration rates were significantly higher from VR9 to the other two sites; however, the sample size at VR9 was low (n = 4).

For all species, we detected a correlation between geographic and genetic distances, which was strongest for *A. fluviatilis* II and weakest for *D. gonocephala* (Figure S4). Genetic diversity (i.e., $H_O$ and AR) differed among sites for all species, but with no consistent pattern over all species (Table S6).

**Effects of in-stream barriers on population structure**

For the analysis of in-stream barrier effects, loci were filtered separately for each barrier site, mostly resulting in a greater number of variable loci and increased genetic diversity per barrier sites in comparison to the total dataset (Table S7). For seven of nine weirs and six of eight culverts, we found no evidence for a barrier effect on population structure in any species. This means that populations at barrier sites were either i) not differentiated at all, ii) differentiation was similar among reference and barrier separated sites, iii) lower for some of the comparisons of barrier separated sites compared to reference sites, or iv) that only single sampling sites were constantly differentiated to the other sites from the same barrier site. All these four differentiation patterns were found for all species. Differentiation between single sites was most prominent for specimens sampled in side streams (“N”;

Figure 8A), despite the lack of obvious barriers. For three weirs, reduced migration rates were detected for *A. fluviatilis* I and II (QB11, QB12 and QB17) in upstream direction across the barrier (Figure 8B); however, this barrier effect was not supported by other analyses and accordingly was not considered in subsequent analyses. A similar reduction was observed for VR6a for *D. gonocephala*; however, the sample size was too small at upstream sites (Figure 8B).

We only detected distinct barrier effects associated with weirs for *D. gonocephala* at QB24 and QB11. In both cases, differentiation across barriers was larger than that between reference sites (Figure 8A). The effect was stronger for QB24 than for QB11, consistent with the sNMF results, where two clusters were the most probable for QB24. Only the first cluster was found upstream of the barrier, both clusters were found downstream of the barrier, and some specimens showed mixed assignment to both clusters. However, specimens showing high membership to the second cluster were all classified as potential triploids. At both barriers, migration rates in up- and downstream directions were lower across barriers than among reference sites (Figure 8B). For QB24, all rates across the barrier were significantly asymmetric, with stronger downstream dispersal. Further, genetic diversity was higher for both barriers at sites downstream of the barrier, where there were more private alleles in comparison to upstream populations (Tables S8 and S9).

For culverts, we found evidence for a barrier effect on population structure for *A. fluviatilis* II at VR20 and for *A. fluviatilis* III at VR6b. While VR6b was a pipe, VR20 was a combination of a pipe and tunnel with an additional steep drop within, and two streams were joined within the tunnel. At VR20 S4, we only found one specimen belonging to *A. fluviatilis* II, which was excluded from analyses of $F_{ST}$ and migration rate. The other 11 specimens at this site were identified as *A. fluviatilis* I, which was not detected upstream of the culvert. All single-site comparisons across the culvert in *A. fluviatilis* II indicated significant differentiation, including comparisons of both N1 and N2 with S2, which were separated by a pipe and part of the tunnel, while differentiation among reference sites was not significant. In the sNMF analysis, indications for a barrier effect were found with the lowest CE for three clusters. Specimens from both N1 and N2 were split into two clusters (k1: n = 10, k2: n = 6), S1 specimens were assigned to k2 or the third cluster (k2 = 6, k3=5), and specimens at S3 were

assigned to all three clusters, indicating that downstream dispersal was possible. This pattern was also detected in the divMigrate analysis. Upstream migration across the culvert to both ends was highly reduced, while downstream migration rates were similar or even higher than those among reference sites (Figure 8B). AR was lowest at S2; otherwise, genetic diversity was similar (Tables S8 and S9).

At barrier site VR6, the second and longer pipe caused population differentiation in *A. fluviatilis* III, as all comparisons across the pipe were significant and $F_{ST}$ values were higher than those between reference sites (Figure 8A). These differentiation patterns were supported by the sNMF analysis, where three clusters were detected. Only one cluster was found in S3&4, while the other two were mainly found in S1&2 and less frequently in S3&4, where assignment to multiple clusters was observed. While migration rates between sites were generally reduced, upstream migration across the second pipe (VR6b) was even more strongly reduced to nearly zero. By contrast, migration rates across the first pipe (VR6a) were even higher than those among reference sites (Figure 8B). $H_O$ was similar at all sampling sites, while AR and the number of private alleles were higher at S3&4 than at other sites (Tables S8 and S9). Unlike in *D. gonocephala* and *A. fluviatilis*, we did not detect evidence for a barrier effect on population structure in *G. fossarum* at any of the barriers.

**Population genetic simulation**

The simulation of a complete barrier (i.e., no up- or downstream dispersal across the barrier) revealed the quick emergence of strong population differentiation, as determined by increases in $F_{ST}$ values and decreases in migration rates over time (Figure S6, Table S10). In general, barrier effects were similar, independent of the distance between populations. In smaller populations, fluctuations over time were larger, leading to significant population differentiation between reference populations not separated by a barrier. However, after only a few generations, $F_{ST}$ values for populations separated by a barrier were consistently higher than those between reference populations. For larger populations, it took up to 50 generations to detect differentiation and $F_{ST}$ values remained low but followed the same general pattern (Figure S6). Only $F_{ST}$ values between populations separated by a barrier were significant. The higher the extinction rate, the higher the $F_{ST}$ values between barrier-separated populations and also in

larger populations, differentiation was detected earlier. For smaller populations with higher extinction rates, significant differentiation was detected without a barrier but remained lower than for barrier-separated populations. These patterns were visible for all tested migration matrices, with asymmetric matrices leading, on average, to slightly higher $F_{ST}$ values. Applying different selfing rates to simulate hermaphrodites, $F_{ST}$ values increased with increasing selfing rates, but patterns were generally the same as those for populations with obligate sexual reproduction. Even though complete isolation between populations on both sides of the barrier was not directly detected, a reduction in migration rates after barrier introduction was quickly (<10 generations) detected for all migration scenarios and decreased further with time. The reduction was more easily detected for larger sample sizes, higher extinction rates and smaller populations.

In general, barriers impeding upstream but not downstream dispersal did not affect the population structure and did not result in constantly reduced migration rates (Figure S6, Table S10). At some time points for small populations (particularly in combination with higher extinction and/or selfing rates), $F_{ST}$ values were slightly higher and significant for barrier-separated populations than for reference populations, but this pattern fluctuated over generations and did not increase with time (similar to migration rate estimates). Reducing downstream dispersal rates led to an intermediate pattern between those described previously. Not all parameter combinations were simulated, but downstream dispersal rates had to be reduced substantially to influence population differentiation. The effects were stronger (and sometimes only detectable) for smaller population sizes, higher extinction or selfing rates, and were strongest for a combination of these parameters (i.e., if population sizes were small and extinction rates were high). If the selfing rate was increased from 0.3 to 0.6, the effect on the population structure was generally high but barrier effects were less detectable because fluctuations between populations and over generations were higher. We obtained similar results for migration rates. $H_O$ and AR were, in general, not affected by the barrier model (Figure S7). Both AR and $H_O$ decreased more strongly over time for smaller population sizes and higher extinction proportions for all dispersal models (with no or slow decreases for larger population sizes, i.e., 1000 and 2000).

However, the decrease was constant over time, independent of the introduction of a barrier into the system, and was similar in all populations.

## Discussion

For all five stream species, our population genomic data revealed strong population differentiation at local scales, with gene flow strongly impeded after ~10 km, especially for *G. fossarum* and *D. gonocephala*. However, we found little evidence that the tested in-stream barriers contributed to population fragmentation. At only two weirs for *D. gonocephala* and one culvert each for *A. fluviatilis* II and III, we detected a significant fragmentation effect. This raises the questions of whether barrier effects are detectable by the chosen methods for barriers between 33 and 109 years old, and whether it is possible to detect an effect when only upstream dispersal is impeded. Further, differences in life history traits can influence the strength of barrier effects on population structure.

Hence, we simulated population genetic null models under specific life history traits to assess the timescale of barrier effect detectability in population genetic data. The simulation results showed that barriers preventing up- as well as downstream dispersal across barriers will lead to strong population structure relatively quickly (i.e., within the age range of the barriers tested), which is detectable by the analysis methods used in this study. The time until effects were detectable was dependent on the population size and extinction rates, with smaller populations showing barrier-related structure already after 5 to 20 generations. In small populations, population differentiation was also detected between reference populations but was already after few generations higher among barrier-separated populations. This highlights the importance of including reference populations in analyses of barrier effects. Simulations preventing only upstream dispersal revealed no effect on population structure for any of the analysis methods. When downstream dispersal was reduced, barrier effects were detectable if populations were small, particularly when extinction and/or selfing rates were high. However, with high selfing rates, fluctuations between populations and over generations were increased, hampering detectability.

Considering different population genetic estimates, simulations indicated that reduced $H_O$ or AR could not be used to detect barrier effects, as both genetic diversity measures decreased constantly over time in small reference and barrier-separated populations, or remained relatively constant in larger populations. For our study design, level of $F_{ST}$ and the number of pairwise comparisons with significant divergence between reference and barrier-separated populations were the most reliable indicators of migration barriers. With migration rates estimated by divMigrate, complete barriers were detectable as well by a general reduction in migration rates between barrier-separated sites. However, in general, migration rates were overestimated, suggesting that low migration rates in real data are probably reliable for analyses of barrier effects.

To conclude, simulations showed that even minor migration in one direction is sufficient to counteract barrier-related population differentiation, especially for large effective population sizes. In large populations, genetic differentiation also remained low over a long time, even if migration between populations was prevented. Accordingly, reduced migration due to barriers is expected to be detectable if migration rates are low, but detection will be difficult or not possible for very young (<10 years) barriers, for barriers only reducing upstream dispersal and for large effective population sizes.

We hypothesised that effects would depend on the severity of the barrier and would be strongest for *A. fluviatilis*, intermediate for *D. gonocephala* and lowest for *G. fossarum*. These hypotheses were only partially supported by our analyses. For only single species at a few barriers characterised as most severe, we detected a stronger population structure and reduced migration rates compared to those for reference populations. For most weirs and culverts, no effect was found, indicating that all species are in principle able to overcome the tested small in-stream barriers frequent enough (or at least in one direction) to facilitate gene flow. As expected, the effects were weakest for *G. fossarum* clade 11, indicating that the dispersal ability is high enough to overcome the small in-stream barriers (see also Weiss & Leese, 2016), congruent with findings for *G. fossarum* clade 12 (Alp et al., 2012). It is also possible that the tested barriers were not old enough to create detectable isolation patterns (Monaghan, Spaak, Robinson, & Ward, 2001) or that the reduction in migration was not strong enough to impact population structure determined by the genetic markers (Whiterod et al., 2017).

However, based on the barrier ages (>30 years), distinct local population structure and simulation results, these explanations are unlikely.

Our prediction that barrier effects would be moderate for *D. gonocephala* and strongest for *A. fluviatilis* was not supported by the data. Only two weirs and two culverts had species-specific barrier effects. The weirs influencing *D. gonocephala* were classified as the second (QB24) and third (QB11) most severe according to height, steepness and smoothness. They were both >80 years old. For other barriers of the same age, no population structure was detected. For QB24, relatively high $F_{ST}$ values were detected between barrier-separated populations. While both up- and downstream migration rates were lower than those between reference sites, migration was significantly stronger downstream than upstream of the barrier. By contrast, for QB27, which was even higher than QB24 with a smoother ramp slope, no effect was detected. The difference between barriers of the same age might be explained by the difference in population size or that important barrier characteristics had not been measured. A weaker effect was detected at QB11 than at QB24; QB11 was not as high and had a moderate slope with drops at the start and the end, which could have strengthened the effect in comparison with other barriers with similar slope. Our results indicate that *D. gonocephala* maintains gene flow over most small weirs, but weirs of the size and shape tested can impede migration. Contrary to our expectations, *A. fluviatilis* migration was not stronger affected by weirs. At three weirs, upstream migration rates detected across barriers were lower than those at reference sites; however, weirs did not affect population structure. In some cases, migration was generally reduced (i.e., also between reference sites). To finally conclude that small weirs do not influence migration in *A. fluviatilis*, it would be important to increase the sample size and to evaluate the influence of polyploidy on analyses.

For culverts, patterns were more consistent with our expectations. We only detected effects for *A. fluviatilis* II and III at two culverts predicted to have the strongest impact (VR20 and VR6b). At VR20, only *A. fluviatilis* II was found upstream of the culvert, while *A. fluviatilis* I was additionally found at downstream sites. While downstream dispersal seemed to be possible through this culvert, upstream dispersal was highly limited. A similar pattern was found for *A. fluviatilis* III at VR6b, even

though here, inferred dispersal in both directions was reduced also between reference sites, but more strongly across the longer of the two pipes analysed at this barrier site. For the other species, we could not attribute observed population structure between sampling sites to the pipes or the sample size upstream of the barrier was too small *(D. gonocephala*). These results indicate that all studied species can probably disperse effectively through tunnels of up to 120 m long, but pipes can act as strong dispersal barriers probably due to their smooth internal structures and high flow velocity (David et al., 2014) or drops, preventing upstream movement (Vaughan, 2002). In general, single small barriers did not have a large impact on population structure, yet it remains to be determined whether population structure increases when many barriers occur within short distances.

**Regional subdivision**

In contrast to minor barrier effects on population structure, differentiation between streams was high for all species. In view of the predicted life history patterns, we hypothesised that population structure would be weakest for *G. fossarum*, intermediate for *D. gonocephala*, and greatest for *A. fluviatilis.* Contrary to our expectation, *G. fossarum* showed the highest population differentiation and the lowest migration rates between populations, *A. fluviatilis* species showed the lowest differentiation and *D. gonocephala* showed an intermediate level of differentiation. For *G. fossarum*, populations were clustered according to streams. At the shortest distances of 11–14 km, populations were already highly differentiated, with $F_{ST}$ values of approximately 0.35. Analysing populations sampled at sites approximately 2 km apart within a single stream showed that gene flow in *G. fossarum* is possible over this distance ($F_{ST}$ for QB17/23: 0.01) but can already be reduced ($F_{ST}$ for VR6/VR17: 0.15). In contrast to the other species, we detected strong phylogeographic structure. Populations clustered into three groups in a network analysis, congruent with the geographic distribution and mitochondrial COI groups defined by Weiss & Leese (2016), indicating that the area was probably recolonised by at least three distinct historical source populations. This strong influence of historical processes on population differentiation could explain the higher population differentiation in comparison to that in the other species. Still, the strong differentiation after 10 km is inconsistent with the relatively high mobility,

locally large populations and regionally broad distribution. It is possible that the dispersal ability is lower than expected or, more likely, that unidentified dispersal barriers exist. These barriers could be human-induced alterations and fragmentations, such as large dams, weirs and culverts (especially larger pipes), or unfavourable conditions in connecting areas, such as those caused by anthropogenic land use, organic pollution, acidification or large connecting rivers (e.g., Alp et al., 2012; Cook et al., 2007; Monaghan et al., 2001; Watanabe et al., 2010). Furthermore, gene flow does correspond directly with individual movements of specimens (e.g., Bohonak & Jenkins, 2003) when dispersing individuals are not able to successfully establish in an existing population. This phenomenon is described by the monopolisation hypothesis (e.g., De Meester et al., 2002), which predicts that adaptation along with the numerical advantage of first migrants leads to a priority effect of the founder population over new migrants and therefore reduces establishment success. Such intraspecific priority effects as well as isolation by adaptation patterns have been detected in various taxa (e.g., Boileau et al., 1992; Fraser et al., 2014; Nosil et al., 2008; Urban & De Meester, 2009) and could have led to increased differentiation.

In *D. gonocephala*, we detected fairly high population differentiation, with isolation between populations inhabiting different streams. In contrast to *G. fossarum*, no strong geographic structure was found, supported by the low IBD pattern. Populations separated by only approximately 2 km in the same stream showed significant population differentiation ($F_{ST}$ 0.07 and 0.11). Differentiation was also detected for 11 to 18 km but was not correlated with waterway distance within this range, suggesting that additional factors other than waterway distance influence effective migration in this species. Local adaptation could shape the population structure, as reported for a population in the same study area in response to high copper concentrations (Weigand et al., 2018), in which high population differentiation was found. Apart from this, little is known about effective dispersal in *D. gonocephala*, but planarians are generally been regarded as weak dispersers (e.g., Rader et al., 2017). A strong population structure across small spatial scales has been found for the freshwater planarians *Crenobia alpina* (Brändle, Heuser, Marten, & Brandl, 2007) and *Polycelis coronata* (Rader et al., 2017). By contrast, low divergence in the COI gene over great geographic distances has been found for

*Schmidtea polychroa* (Pongratz, Storhas, Carranza, & Michiels, 2003) and *Dugesia sicula* (Lázaro & Riutort, 2013), interpreted as strong dispersal ability of these species. The overall lower $F_{ST}$ values than those for *G. fossarum* could indicate that *D. gonocephala* is a better disperser. However, it is more likely that differences in $F_{ST}$ reflect the greater phylogenetic signal in *G. fossarum*, represented by three deep phylogenetic lineages as described above. In *D. gonocephala*, particularly strong population structure in some cases was associated with the presence of triploid individuals. Triploids originating from different streams did not cluster together but were closely related to specimens in the same stream, indicating that polyploidy evolved independently several times. Still results concerning possible polyploid individuals have to be interpreted cautiously, because it is difficult to assess how analyses are affected for example by allelic dosage uncertainty (Dufresne et al., 2014). Further, because we estimated ploidy levels only indirectly, we cannot say if individuals are really triploids or aneuploids with high chromosome numbers as it has been implied for a French *D. gonocephala* population (de Vries, 1986). Therefore, chromosome numbers in respective populations should be analysed by karyograms or other approaches. At sites with triploids, they often made up the majority, consistent with previous results showing that asexual polyploids are more abundant than diploids (Álvarez-Presas & Riutort, 2014). Asexual populations of *D. gonocephala* have not been reported (Stocchino & Manconi, 2013), but we cannot exclude the possibility and polyploid populations should be analysed in more detail in future studies.

The low genetic structure in *A. fluviatilis* species could be explained by the presence of three relatively young cryptic species in the area (see Weiss et al., 2018 for details), as time since speciation might have been not long enough to generate similar variation compared to e.g. the extremely diverse *G. fossarum*. Further, analyses were complicated by the polyploid genomes. The chosen analysis approaches should still be able to generate reliable results concerning population genetic (Dufresne et al., 2014), but also loci detection could have been influenced by the ploidy. Even though we chose the most rigorous Stacks settings to disentangle homoeologous loci of different genomes, observed heterozygosity, particularly for *A. fluviatilis* II, was still much higher than those for *D. gonocephala* and *G. fossarum*. Even though this filtering was necessary, it led to fewer loci being analyzed for the

different *A. fluviatilis* taxa. Despite the lower population structure, significant differentiation between populations originating from different streams and generally low migration rates among populations were detected for all *A. fluviatilis* species, and a high number of genetic clusters was supported by the sNMF analyses. Additionally, most within-stream comparisons showed low but significant differentiation, even within a few hundred meters. In general, our findings suggest that effective dispersal is low between streams and differentiation within streams can occur over short distances (see also Macher, Weiss, Beermann, & Leese, 2016). In some cases, we detected genetic structure within barrier sites, while in other cases, levels of shared ancestry were higher than those for *G. fossarum* or *D. gonocephala*. This may reflect higher occasional gene flow between streams, a younger recolonisation history, or could have been influenced by polyploidy and the still high heterozygosity in the data set. For a better understanding of the determinants of population structure, it is important to better characterise homoeologous loci and to determine ploidy levels of individuals. However, the consistent overall patterns across species suggest that our results are reliable, and population isolation in the absence of differences in dispersal capacity indicates that strong dispersal barriers exist in the area, which are not identified, yet.

## Conclusions

In summary, we detected genetic isolation among populations of five hololimnic species between streams and found that effective dispersal was low even across local-scale waterway distances. The highly resolved genomic ddRAD data showed that single small weirs and culverts are probably not the cause of population fragmentation. Therefore, further studies are needed to identify the key barriers. In general, our combination of genomic markers, population genetic simulations and a controlled sampling design with distinct reference populations is a suitable tool to infer major drivers of regional and local population structure.

## Acknowledgements

We thank Lisa Pöttker, Markus Patschke, Vivienne Dobrzinski, Janis Neumann and Tobias Traub for assistance with sampling; Ralph Tollrian for support; and Romana Salis for helpful comments on the manuscript. Furthermore, we thank Jörg Drewenskus (Bezirksregierung Arnsberg) for information on barrier ages and LANUV for further information on sampling sites. We especially thank Johannes Köster for help creating Snakemake workflows. The project was funded by the Kurt Eberhard Bode Foundation within the Deutsches Stiftungszentrum.

**Data Availability**

ddRAD data for *G. fossarum* and *D. gonocephala* will be available at NCBI BioProject upon publication. ddRAD data for *A. fluviatilis* I, II and III will be available at NCBI BioProject with accession number PRJNA389679. Snakemake workflows, python and R-Scripts will be available at BitBucket.

## References


Alp, M., Keller, I., Westram, A., & Robinson, C. (2012). How river structure and biological traits influence gene flow: A population genetic study of two stream invertebrates with differing dispersal abilities. *Freshwater Biology*, *57*, 969–981. doi: 10.1111/j.1365-2427.2012.02758.x

Álvarez-Presas, M., & Riutort, M. (2014). Planarian (Platyhelminthes, Tricladida) Diversity and Molecular Markers: A New View of an Old Group. *Diversity*, *6*(2), 323–338. doi: 10.3390/d6020323

Baršiene, J., Tapia, G., & Barsyte, D. (1996). Chromosomes of molluscs inhabiting some mountain springs of eastern Spain. *Journal of Molluscan Studies*, *62*(4), 539–543. doi: 10.1093/mollus/62.4.539

Bijlsma, R., & Loeschcke, V. (2012). Genetic erosion impedes adaptive responses to stressful environments. *Evolutionary Applications*, *5*(2), 117–129. doi: 10.1111/j.1752-4571.2011.00214.x

Bohonak, A., & Jenkins, D. (2003). Ecological and evolutionary significance of dispersal by freshwater invertebrates. *Ecology Letters*, *6*, 783–796. doi: 10.1046/j.1461-0248.2003.00486.x

Boileau, M. G., Hebert, P. D. N., & Schwartz, S. S. (1992). Non□equilibrium gene frequency divergence: Persistent founder effects in natural populations. *Journal of Evolutionary Biology*, *5*(1), 25–39. doi: 10.1046/j.1420-9101.1992.5010025.x

Brändle, M., Heuser, R., Marten, A., & Brandl, R. (2007). Population structure of the freshwater flatworm *Crenobia alpina* (Dana): Old lineages and low gene flow. *Journal of Biogeography*, *34*(7), 1183–1192. doi: 10.1111/j.1365-2699.2007.01689.x

Brittain, J., & Eikeland, T. (1988). Invertebrate drift—A review. *Hydrobiologia*, *166*, 77–93.

Bryant, D., & Moulton, V. (2004). Neighbor-Net: An Agglomerative Method for the Construction of Phylogenetic Networks. *Molecular Biology and Evolution*, *21*(2), 255–265. doi: 10.1093/molbev/msh018

Burch, J. B. (1962). Chromosome numbers and systematics in euthyneuran snails. *Proceedings of the First European Malacological Congress*, 215–241.

Catchen, J. M., Hohenlohe, P. A., Bassham, S., Amores, A., & Cresko, W. A. (2013). Stacks: An analysis tool set for population genomics. *Molecular Ecology*, *22*(11), 3124–3140. doi: 10.1111/mec.12354

Coleman, R. A., Gauffre, B., Pavlova, A., Beheregaray, L. B., Kearns, J., Lyon, J., … Sunnucks, P. (2018). Artificial barriers prevent genetic recovery of small isolated populations of a low-mobility freshwater fish. *Heredity*, *120*(6), 515–532. doi: 10.1038/s41437-017-0008-3

Cook, B., Bunn, S., & Hughes, J. (2007). A comparative analysis of population structuring and genetic diversity in sympatric lineages of freshwater shrimp (Atyidae: *Paratya*): Concerted or independent responses to hydrographic factors? *Freshwater Biology*, *52*, 2156–2171. doi: 10.1111/j.1365-2427.2007.01842.x

David, B. O., Tonkin, J. D., Taipeti, K. W. T., & Hokianga, H. T. (2014). Learning the ropes: Mussel spat ropes improve fish and shrimp passage through culverts. *Journal of Applied Ecology*, *51*(1), 214–223. doi: 10.1111/1365-2664.12178

De Meester, L., Gómez, A., Okamura, B., & Schwenk, K. (2002). The Monopolization Hypothesis and the dispersal–gene flow paradox in aquatic organisms. *Acta Oecologica*, *23*, 121–135.

de Vries, E. J. (1986). On the karyology of *Dugesia gonocephala* s.l. (Turbellaria, Tricladida) from Montpellier, France. *Hydrobiologia*, *132*(1), 251–256. doi: 10.1007/BF00046257

Dillon, R. T. (1988). The influence of minor human disturbance on biochemical variation in a population of freshwater snails. *Biological Conservation*, *43*(2), 137–144. doi: 10.1016/0006-3207(88)90087-0

Dufresne, F., Stift, M., Vergilino, R., & Mable, B. K. (2014). Recent progress and challenges in population genetics of polyploid organisms: An overview of current state-of-the-art molecular and statistical tools. *Molecular Ecology*, *23*(1), 40–69. doi: 10.1111/mec.12581

Dumont, U., Anderer, P., & Schwevers, U. (2005). *Handbuch Querbauwerke*. Düsseldorf: Ministerium für Umwelt und Naturschutz, Landwirtschaft und Verbraucherschutz des Landes Nordrhein-Westfalen.

Eder, E., Hödl, W., Moog, O., Nesemann, H., Pöckl, M., & Wittmann, K. (1995). Crustacea. In *Fauna Aquatica Austriaca Lieferungen 1994, 2002* (Vol. 2002). Wien: Wasserwirtschaftskataster, Bundesministerium für Land- und Forstwirtschaft, Umwelt und Wasserwirtschaft.

Elliott, J. (2003). A comparative study of the dispersal of 10 species of stream invertebrates. *Freshwater Biology*, *48*, 1652–1668.

Fraser, C., Banks, S., & Waters, J. (2014). Priority effects can lead to underestimation of dispersal and invasion potential. *Biological Invasions*, 1–8.

Frichot, E., & François, O. (2015). LEA: An R package for landscape and ecological association studies. *Methods in Ecology and Evolution*, *6*(8), 925–929. doi: 10.1111/2041-210X.12382

Frichot, E., Mathieu, F., Trouillon, T., Bouchard, G., & François, O. (2014). Fast and Efficient Estimation of Individual Ancestry Coefficients. *Genetics*, *196*(4), 973. doi: 10.1534/genetics.113.160572

Goudet, J. (2005). Hierfstat, a package for r to compute and test hierarchical F-statistics. *Molecular Ecology Notes*, *5*(1), 184–186. doi: 10.1111/j.1471-8286.2004.00828.x

Grill, G., Lehner, B., Lumsdon, A. E., MacDonald, G. K., Zarfl, C., & Liermann, C. R. (2015). An index-based framework for assessing patterns and trends in river fragmentation and flow regulation by global dams at multiple scales. *Environmental Research Letters*, *10*(1), 015001. doi: 10.1088/1748-9326/10/1/015001

Guillaume, F., & Rougemont, J. (2006). Nemo: An evolutionary and population genetics programming framework. *Bioinformatics*, *22*(20), 2556–2557. doi: 10.1093/bioinformatics/btl415

Hansen, M. M., Limborg, M. T., Ferchaud, A.-L., & Pujolar, J.-M. (2014). The effects of Medieval dams on genetic divergence and demographic history in brown trout populations. *BMC Evolutionary Biology*, *14*(1), 122. doi: 10.1186/1471-2148-14-122

Hoban, S., Bertorelle, G., & Gaggiotti, O. E. (2012). Computer simulations: Tools for population and

evolutionary genetics. *Nature Reviews Genetics*, *13*(2), 110–122. doi: 10.1038/nrg3130

Horreo, J. L., Martinez, J. L., Ayllon, F., Pola, I. G., Monteoliva, J. A., Héland, M., & Garcia-Vazquez, E. (2011). Impact of habitat fragmentation on the genetics of populations in dendritic landscapes. *Freshwater Biology*, *56*(12), 2567–2579. doi: 10.1111/j.1365-2427.2011.02682.x

Hudman, S. P., & Gido, K. B. (2013). Multi scale effects of impoundments on genetic structure of creek chub (*Semotilus atromaculatus*) in the Kansas River basin. *Freshwater Biology*, *58*(2), 441–453. doi: 10.1111/fwb.12079

Hughes, J., Schmidt, D., McLean, A., & Wheatley, A. (2008). Population genetic structure in stream insects: What have we learned? In J. Lancaster & R. A. Briers (Eds.), *Aquatic Insects: Challenges to Populations: Proceedings of the Royal Entomological Society's 24th Symposium* (pp. 268–288). London: CABI.

Huson, D. H., & Bryant, D. (2006). Application of Phylogenetic Networks in Evolutionary Studies. *Molecular Biology and Evolution*, *23*(2), 254–267. doi: 10.1093/molbev/msj030

Jackson, R. B., Carpenter, S. R., Dahm, C. N., McKnight, D. M., Naiman, R. J., Postel, S. L., & Running, S. W. (2001). Water in a changing world. *Ecological Applications*, *11*(4), 1027–1045. doi: 10.1890/1051-0761(2001)011[1027:WIACW]2.0.CO;2

Junker, J., Peter, A., Wagner, C. E., Mwaiko, S., Germann, B., Seehausen, O., & Keller, I. (2012). River fragmentation increases localized population genetic structure and enhances asymmetry of dispersal in bullhead (*Cottus gobio*). *Conservation Genetics*, *13*(2), 545–556. doi: 10.1007/s10592-011-0306-x

Keenan, K., McGinnity, P., Cross, T. F., Crozier, W. W., & Prodöhl, P. A. (2013). diveRsity: An R package for the estimation of population genetics parameters and their associated errors. *Methods in Ecology and Evolution*, *4*(8), 782–788. doi: 10.1111/2041-210X.12067

Köster, J., & Rahmann, S. (2012). Snakemake—A scalable bioinformatics workflow engine. *Bioinformatics*, *28*(19), 2520–2522. doi: 10.1093/bioinformatics/bts480

Lázaro, E. M., & Riutort, M. (2013). *Dugesia sicula* (Platyhelminthes, Tricladida): The colonizing success of an asexual Planarian. *BMC Evolutionary Biology*, *13*, 268. doi: 10.1186/1471-2148-13-268

Macher, J. N., Rozenberg, A., Pauls, S. U., Tollrian, R., Wagner, R., & Leese, F. (2015). Assessing the phylogeographic history of the montane caddisfly *Thremma gallicum* using mitochondrial and restriction-site-associated DNA (RAD) markers. *Ecology and Evolution*, *5*(3), 648–662. doi: 10.1002/ece3.1366

Macher, J. N., Weiss, M., Beermann, A. J., & Leese, F. (2016). Cryptic diversity and population structure at small scales: The freshwater snail *Ancylus* (Planorbidae, Pulmonata) in the Montseny mountain range. *Annales de Limnologie - International Journal of Limnology*, *52*, 387–399. doi: 10.1051/limn/2016026

MacNeil, C., Dick, J., & Elwood, R. (1997). The trophic ecology of freshwater *Gammarus* spp. (Crustacea: Amphipoda): Problems and perspectives concerning the functional feeding group concept. *Biological Reviews*, *72*, 349–364.

Minshall, G. W., & Winger, P. V. (1968). The Effect of Reduction in Stream Flow on Invertebrate Drift. *Ecology*, *49*(3), 580–582. doi: 10.2307/1934133

Monaghan, M., Spaak, P., Robinson, C., & Ward, J. (2001). Genetic differentiation of *Baetis alpinus* Pictet (Ephemeroptera: Baetidae) in fragmented alpine streams. *Heredity*, *86*, 395–403. doi: 10.1046/j.1365-2540.2001.00843.x

Moog, O. (1995). Functional-Feeding Guilds—Family/Genus Level. In *Fauna Aquatica Austriaca, Lieferungen 1995*. Wien: Wasserwirtschaftskataster, Bundesministerium für Land-und Forstwirtschaft.

Nei, M. (1973). Analysis of Gene Diversity in Subdivided Populations. *Proceedings of the National Academy of Sciences*, *70*(12), 3321. doi: 10.1073/pnas.70.12.3321

Nesemann, H., & Reischütz, P. (1995). Gastropoda. In *Fauna Aquatica Austriaca, Lieferungen 1995, 2002*. Wien: Wasserwirtschaftskataster, Bundesministerium für Land- und Forstwirtschaft, Umwelt und Wasserwirtschaft.

Nilsson, C., Reidy, C. A., Dynesius, M., & Revenga, C. (2005). Fragmentation and Flow Regulation of the World's Large River Systems. *Science*, *308*(5720), 405. doi: 10.1126/science.1107887

Nosil, P., Egan, S. P., & Funk, D. J. (2008). Heterogeneous genomic differentiation between walking□stick ecotypes:"isolation by adaptation" and multiple roles for divergent selection. *Evolution*, *62*(2), 316–336. doi: 10.1111/j.1558-5646.2007.00299.x

Oksanen, J., Blanchet, F. G., Friendly, M., Kindt, R., Legendre, P., McGlinn, D., … Wagner, H. (2019). *vegan: Community Ecology Package*. Retrieved from https://CRAN.R-project.org/package=vegan

Paris, J. R., Stevens, J. R., & Catchen, J. M. (2017). Lost in parameter space: A road map for STACKS. *Methods in Ecology and Evolution*. doi: 10.1111/2041-210X.12775

Patrick, C. J., Cooper, M. J., & Uzarski, D. G. (2014). Dispersal Mode and Ability Affect the Spatial Turnover of a Wetland Macroinvertebrate Metacommunity. *Wetlands*, *34*(6), 1133–1143. doi: 10.1007/s13157-014-0572-8

Patterson, N., Price, A. L., & Reich, D. (2006). Population Structure and Eigenanalysis. *PLoS Genetics*, *2*(12), e190. doi: 10.1371/journal.pgen.0020190

Peterson, B. K., Weber, J. N., Kay, E. H., Fisher, H. S., & Hoekstra, H. E. (2012). Double Digest RADseq: An Inexpensive Method for De Novo SNP Discovery and Genotyping in Model and Non-Model Species. *PLOS ONE*, *7*(5), e37135. doi: 10.1371/journal.pone.0037135

Pongratz, N., Storhas, M., Carranza, S., & Michiels, N. K. (2003). Phylogeography of competing sexual and parthenogenetic forms of a freshwater flatworm: Patterns and explanations. *BMC Evolutionary Biology*, *3*, 23. doi: 10.1186/1471-2148-3-23

R Core Team. (2015). R: A Language and Environment for Statistical Computing. *R Foundation for Statistical Computing, Vienna, Austria.*, https://www.R-project.org/.

Rader, R. B., Unmack, P. J., & Moore, J. N. (2017). Population genetics and dispersal of the flatworm, *Polycelis coronata*: A test of the habitat stability hypothesis. *Journal of Freshwater Ecology*, *32*(1),

179–192. doi: 10.1080/02705060.2016.1253624

Resh, V. H. (2005). Stream crossings and the conservation of diadromous invertebrates in South Pacific island streams. *Aquatic Conservation: Marine and Freshwater Ecosystems*, *15*(3), 313–317. doi: 10.1002/aqc.644

Schmidt-Kloiber, A., & Hering, D. (2015). Www. Freshwaterecology. Info–An online tool that unifies, standardises and codifies more than 20,000 European freshwater organisms and their ecological preferences. *Ecological Indicators*, *53*, 271–282.

Stocchino, G. A., & Manconi, R. (2013). Overview of life cycles in model species of the genus *Dugesia* (Platyhelminthes: Tricladida). *Italian Journal of Zoology*, *80*(3), 319–328. doi: 10.1080/11250003.2013.822025

Sundqvist, L., Keenan, K., Zackrisson, M., Prodöhl, P., & Kleinhans, D. (2016). Directional genetic differentiation and relative migration. *Ecology and Evolution*, *6*(11), 3461–3475. doi: 10.1002/ece3.2096

Tonkin, J. D., Stoll, S., Sundermann, A., & Haase, P. (2014). Dispersal distance and the pool of taxa, but not barriers, determine the colonisation of restored river reaches by benthic invertebrates. *Freshwater Biology*, *59*(9), 1843–1855. doi: 10.1111/fwb.12387

Torterotot, J.-B., Perrier, C., Bergeron, N. E., & Bernatchez, L. (2014). Influence of Forest Road Culverts and Waterfalls on the Fine-Scale Distribution of Brook Trout Genetic Diversity in a Boreal Watershed. *Transactions of the American Fisheries Society*, *143*(6), 1577–1591. doi: 10.1080/00028487.2014.952449

Urban, M., & De Meester, L. (2009). Community monopolization: Local adaptation enhances priority effects in an evolving metacommunity. *Proceedings of the Royal Society B: Biological Sciences*, *276*, 4129–4138.

Van Leeuwen, C. H. A., Dalen, K., Museth, J., Junge, C., & Vøllestad, L. A. (2018). Habitat fragmentation has interactive effects on the population genetic diversity and individual behaviour of a freshwater salmonid fish. *River Research and Applications*, *34*(1), 60–68. doi: 10.1002/rra.3226

Vaughan, D. M. (2002). Potential impact of road-stream crossings (culverts) on the upstream passage of aquatic macroinvertebrates. In *U.S. Forest Service Report*. Portland, Oregon.

Vendrami, D. L. J., Telesca, L., Weigand, H., Weiss, M., Fawcett, K., Lehman, K., … Hoffman, J. I. (2017). RAD sequencing resolves fine-scale population structure in a benthic invertebrate: Implications for understanding phenotypic plasticity. *Royal Society Open Science*, *4*(2). doi: 10.1098/rsos.160548

Vörösmarty, C. J., McIntyre, P. B., Gessner, M. O., Dudgeon, D., Prusevich, A., Green, P., … Davies, P. M. (2010). Global threats to human water security and river biodiversity. *Nature*, *467*(7315), 555.

Vrijenhoek, R. C. (1998). Conservation genetics of freshwater fish. *Journal of Fish Biology*, *53*(sA), 394–412. doi: 10.1111/j.1095-8649.1998.tb01039.x

Watanabe, K., Monaghan, M., Takemon, Y., & Omura, T. (2010). Dispersal ability determines the genetic effects of habitat fragmentation in three species of aquatic insect. *Aquat Conserv Mar Freshw*

*Ecosyst*, *20*. doi: 10.1002/aqc.1124

Weigand, H., Weiss, M., Cai, H., Li, Y., Yu, L., Zhang, C., & Leese, F. (2018). Fishing in troubled waters: Revealing genomic signatures of local adaptation in response to freshwater pollutants in two macroinvertebrates. *Science of the Total Environment*, *633*, 875–891.

Weir, B., & Cockerham, C. (1984). Estimating F-statistics for the analysis of population structure. *Evolution*, *38*, 1358–1370. doi: 10.2307/2408641

Weiss, M., & Leese, F. (2016). Widely distributed and regionally isolated! Drivers of genetic structure in *Gammarus fossarum* in a human-impacted landscape. *BMC Evolutionary Biology*, *16*(1), 153. doi: 10.1186/s12862-016-0723-z

Weiss, M., Macher, J. N., Seefeldt, M. A., & Leese, F. (2014). Molecular evidence for further overlooked species within the *Gammarus fossarum* complex (Crustacea: Amphipoda). *Hydrobiologia*, *721*, 165–184. doi: 10.1007/s10750-013-1658-7

Weiss, M., Weigand, H., Weigand, A. M., & Leese, F. (2018). Genome-wide SNP data reveal cryptic species within cryptic freshwater snail species—The case of the *Ancylus fluviatilis* species complex. *Ecology and Evolution*, *8*(2), 1063–1072. doi: 10.1002/ece3.3706

Wheeler, A. P., Angermeier, P. L., & Rosenberger, A. E. (2005). Impacts of New Highways and Subsequent Landscape Urbanization on Stream Habitat and Biota. *Reviews in Fisheries Science*, *13*(3), 141–164. doi: 10.1080/10641260590964449

Whiterod, N. S., Zukowski, S., Asmus, M., Gilligan, D., & Miller, A. D. (2017). Genetic analyses reveal limited dispersal and recovery potential in the large freshwater crayfish *Euastacus armatus* from the southern Murray–Darling Basin. *Marine and Freshwater Research*, *68*(2), 213–225. doi: 10.1071/MF16006

Zarfl, C., Lumsdon, A. E., Berlekamp, J., Tydecks, L., & Tockner, K. (2015). A global boom in hydropower dam construction. *Aquatic Sciences*, *77*(1), 161–170. doi: 10.1007/s00027-014-0377-0

## Tables

Table 1. Barrier characteristics of culverts (VR) and weirs (QB), sorted by expected severity from high to low

| Name VR/QB | Approx. construction year | Approx. length VR/ height QB [m] | Approx. width × height VR [m] | VR bottom substrate/ QB quality structure | Description of VR/ steepness of QB ramps (low/med/high) |
|---|---|---|---|---|---|
| **VR20** | 1906 (enlarged 1980) | 94/114 | tunnel: 2.5 × 1.2 pipe: ø 0.6 | concrete | tunnel (94 m) between N2 and S3 with a steep drop; S2 joins tunnel via ~30 m-long pipe over small ramp upstream of drop; total length S1–S3: 114 m |
| **VR6b** | 1960 | 22 | ø 0.5 | concrete | 3 parallel concrete pipes, small drop at end |
| **VR6a** | 1960 | 8 | ø 0.5 | concrete | 2 parallel concrete pipes, small drop at end |
| **VR17** | 1980 | 120 | 3 × 1 | artificial sediment | broad tunnel, small drops between S1 & S2 |
| **VR23** | 1910 (enlarged 1970) | 70 | 0.6 × 1 | natural sediment | tunnel |
| **VR12** | – | 38 | 1 × 1.2 | concrete | tunnel |
| **VR11** | 1970 (enlarged 1980) | 34 (72) | 3 × 2 | concrete | big tunnel, up- & downstream 7 small drops |
| **VR9** | 1980 | 56 | 3 × 4 | natural sediment | big tunnel |
| **QB27a** | 1930 | 1.65 | | smooth | high |
| **QB24** | 1930 | 1.5 | | rough | high |
| **QB11** | 1930 | 1.35 | | rough | medium, drops at start and end |
| **QB12** | – | 1.1 | | rough | 1st half medium, 2nd high |
| **QB27b** | 1930 | 1.05 | | smooth | low, drops at start and end |
| **QB22** | 1905 | 1.3 | | rough with bigger stones | medium |
| **QB23** | 1930 | 1.2 | | rough with bigger stones | medium |
| **QB17** | 1960 | 0.6 | | rough | medium |
| **QB20** | – | 1 | | rough | low, small drop at end |

**Figure captions**

Figure 1. Summary of traits differing among studied species. Numbers from 1 to 3 indicate the expected relative gradient. The arrow indicates the expected strength of the barrier effects and population structure.

Figure 2. Central map showing the locations of barrier sites (QB = weirs, VR = culverts). Pie charts indicate sampled species. Water course of sampled streams and main rivers are highlighted. Boxes show the sampling scheme and locations of single sampling sites, with a distance of approx. 200 m. Water flow direction is given by small arrows.

Figure 3. Population genetic structure of *G. fossarum*. A) Ancestry estimates for K = 9, where vertical bars represent individual ancestry coefficients. B) Neighbor-Net, branch colours indicate barrier sites. C) Map of sampling locations. D) DivMigrate plot, strength and visibility of arrows are correlated with migration rates.

Figure 4. Population genetic structure of *D. gonocephala*. A) Ancestry estimates for K = 13, where vertical bars represent individual ancestry coefficients. B) Neighbor-Net, branch colours indicate barrier sites. C) Map of sampling locations. D) DivMigrate plot, strength and visibility of arrows are correlated with migration rates.

Figure 5. Population genetic structure of *A. fluviatilis* I. A) Ancestry estimates for K = 8, where vertical bars represent individual ancestry coefficients. B) Neighbor-Net, branch colours indicate barrier sites. C) Map of sampling locations. D) DivMigrate plot, strength and visibility of arrows are correlated with migration rates.

Figure 6. Population genetic structure of *A. fluviatilis* II. A) Ancestry estimates for K = 8, where vertical bars represent individual ancestry coefficients. B) Neighbor-Net, branch colours indicate barrier sites. C) Map of sampling locations. D) DivMigrate plot, strength and visibility of arrows are correlated with migration rates.

Figure 7. Population genetic structure of *A. fluviatilis* III.
A) Ancestry estimates for K = 4, where vertical bars represent individual ancestry coefficients. B) Neighbor-Net, branch colours indicate barrier sites. C) Map of sampling locations. D) DivMigrate plot, strength and visibility of arrows are correlated with migration rates.

Figure 8. Barrier effects. A) Pairwise $F_{ST}$ values, colored according to presence of barriers. $F_{ST}$ values from site stream populations (N) are shown in different colours. Barriers are ordered according to severity, starting with the strongest weir and strongest culvert. Combi: differentiation across both barriers in one stream. Barriers with detected effect indicated with asterisk. B) Visualisation of migration rates. Only barriers and species for which a possible effect was detected are shown (see Figure S5 for all results). Rates are shown in colours according to the source site, arrows are shown in colours if rates $\Delta \geq 0.15$. Significant asymmetry is indicated by an asterisk. For sample sizes $\leq 3$, rates are shown in lighter colours.

| species | feeding type | reproduction / ploidy | relative population size | relative dispersal capability | predicted strength of barrier effect & population structure |
|---|---|---|---|---|---|
| *G. fossarum* | mainly shredder, (minor also grazer/collector, predator) | sexual / diploid | can have large local populations **1** | dispersal by swimming/ walking, often found in the drift **1** | least affected by barriers & lowest population structure **1** |
| *D. gonocephala* | predator | hermaphrodite, sexual / diploid or aneuploid | as predator smallest population size expected **3** | dispersal by crawling/ swimming possible, rarely found in the drift **2** | mid-level barrier effect & medium differentiation **2** |
| *A. fluviatilis* I, II, III 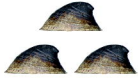 | grazer | hermaphrodite, sexual or asexual / polypoid (different levels possible) | can have large local populations, but smaller than *G. fossarum* **2** | dispersal by crawling/ rarely found in the drift **3** | strongest barrier effect & highest differentiation **3** |

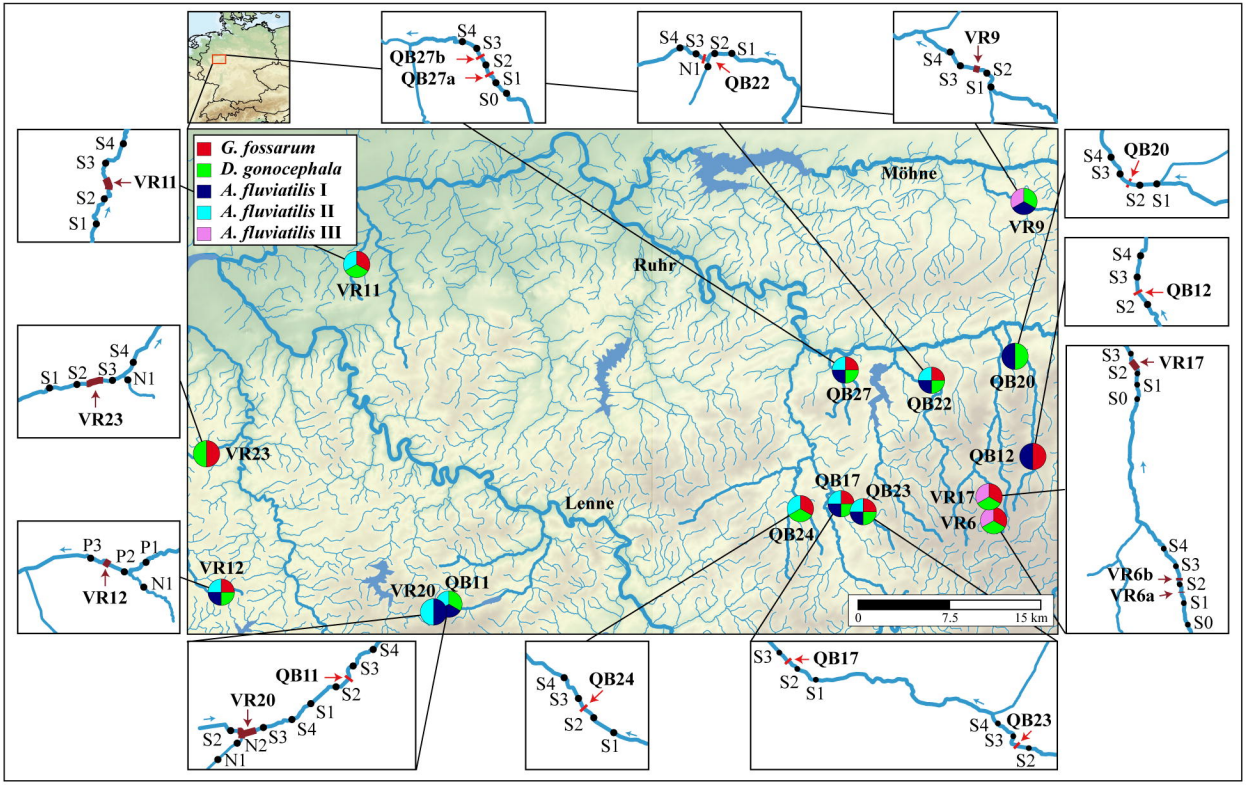
G. fossarum
D. gonocephala
A. fluviatilis I
A. fluviatilis II
A. fluviatilis III
Möhne
Ruhr
Lenne
VR11
VR23
VR12
VR20
QB11
QB27
QB22
QB20
QB12
QB17
QB23
QB24
VR17
VR6
VR9
QB27b
QB27a
QB22
QB20
QB12
VR17
VR6b
VR6a
QB11
QB24
QB17
QB23
0
7.5
15 km

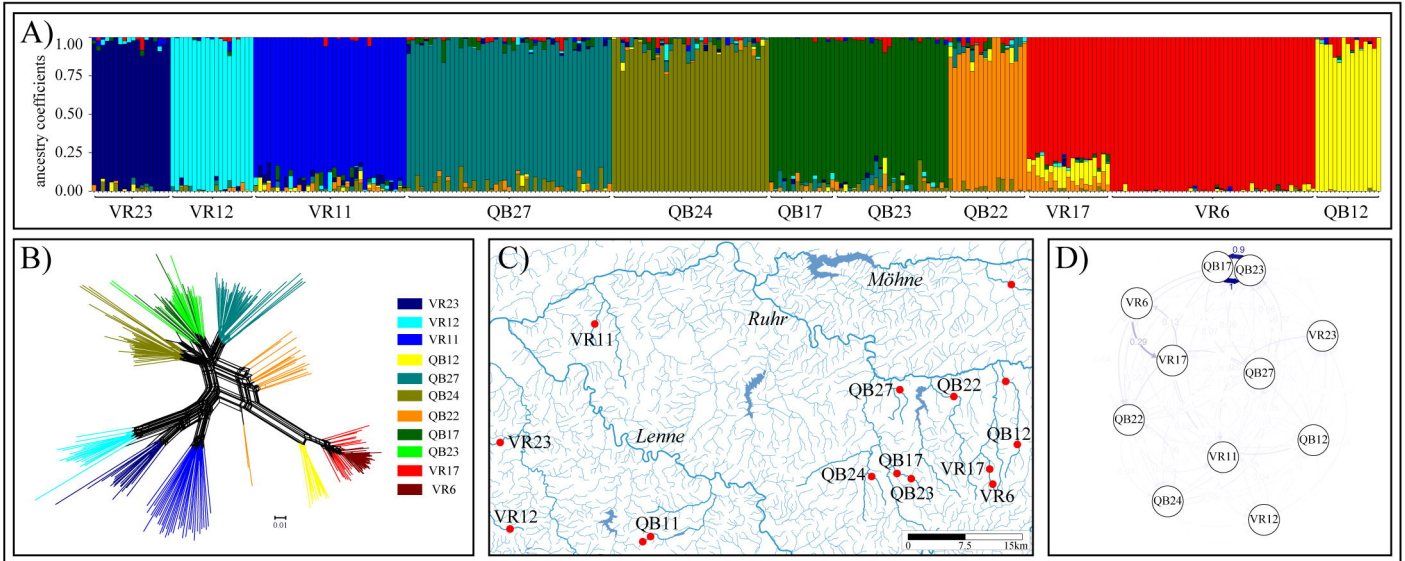
A)
ancestry coefficients
1.00
0.75
0.50
0.25
0.00
VR23
VR12
VR11
QB27
QB24
QB17
QB23
QB22
VR17
VR6
QB12
B)
VR23
VR12
VR11
QB12
QB27
QB24
QB22
QB17
QB23
VR17
VR6
0.01
C)
Möhne
Ruhr
Lenne
VR11
VR23
VR12
QB11
QB27
QB22
QB12
QB24
QB17
QB23
VR17
VR6
0
7.5
15km
D)
0.9
QB17
QB23
VR6
VR23
VR17
QB27
QB22
QB12
VR11
QB24
VR12

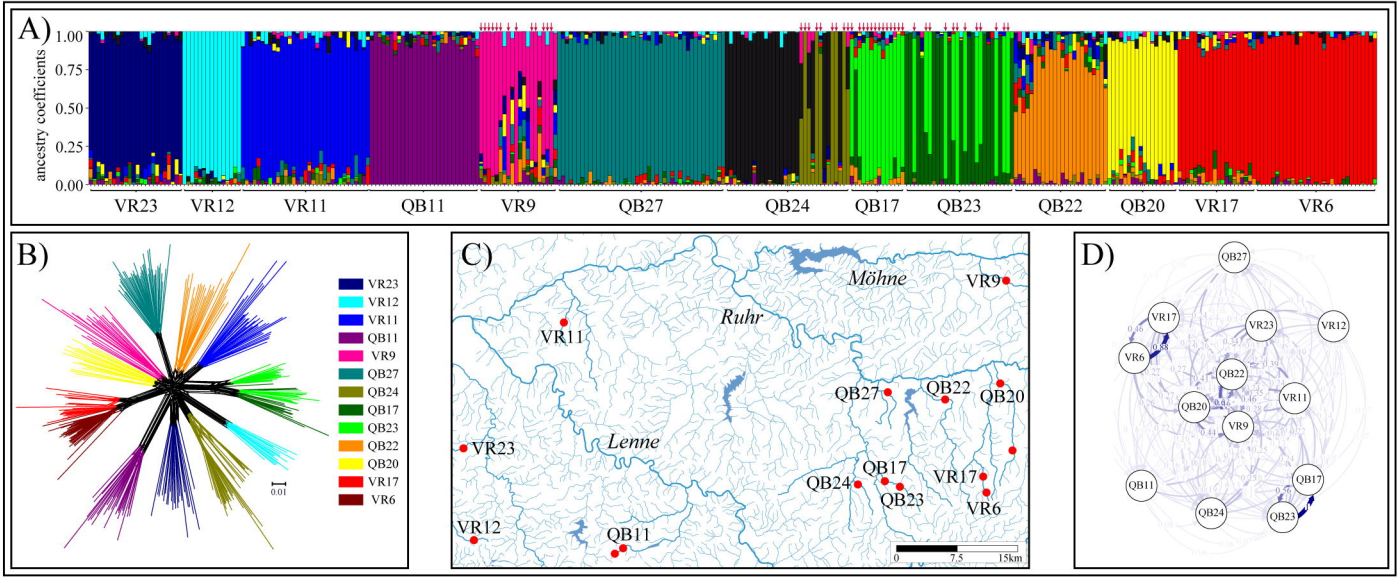
A)
ancestry coefficients
1.00
0.75
0.50
0.25
0.00
VR23
VR12
VR11
QB11
VR9
QB27
QB24
QB17
QB23
QB22
QB20
VR17
VR6
B)
VR23
VR12
VR11
QB11
VR9
QB27
QB24
QB17
QB23
QB22
QB20
VR17
VR6
0.01
C)
Möhne
Ruhr
Lenne
VR9
VR11
QB27
QB22
QB20
VR23
QB17
VR17
QB24
QB23
VR6
VR12
QB11
0
7.5
15km
D)
QB27
VR17
VR23
VR12
VR6
QB22
VR11
QB20
VR9
QB11
QB17
QB24
QB23

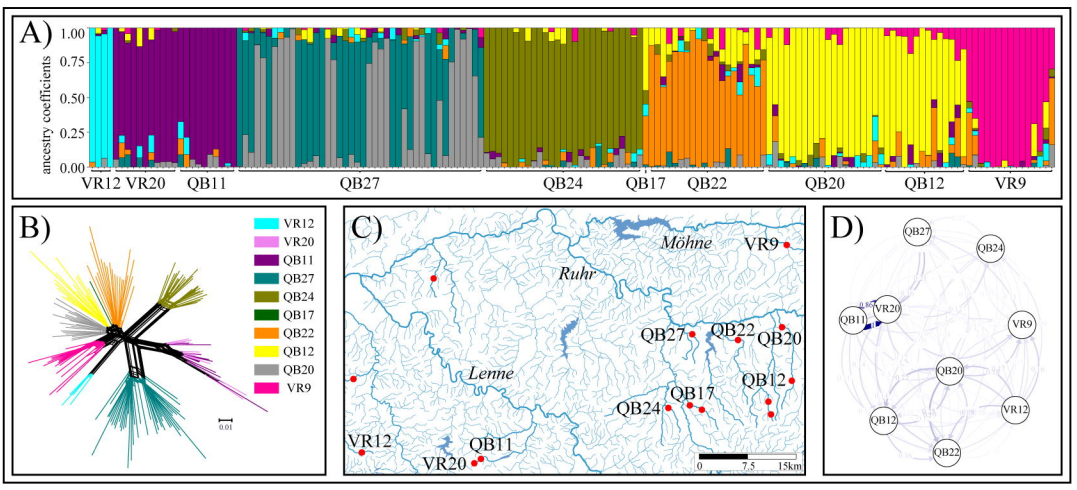
A)
ancestry coefficients
1.00
0.75
0.50
0.25
0.00
VR12 VR20 QB11 QB27 QB24 QB17 QB22 QB20 QB12 VR9
B)
VR12
VR20
QB11
QB27
QB24
QB17
QB22
QB12
QB20
VR9
0.01
C)
Möhne
Ruhr
Lenne
VR9
QB27
QB22
QB20
QB12
QB17
QB24
VR12
QB11
VR20
0
7.5
15km
D)
QB27
QB24
QB11
VR20
VR9
QB20
VR12
QB12
QB22

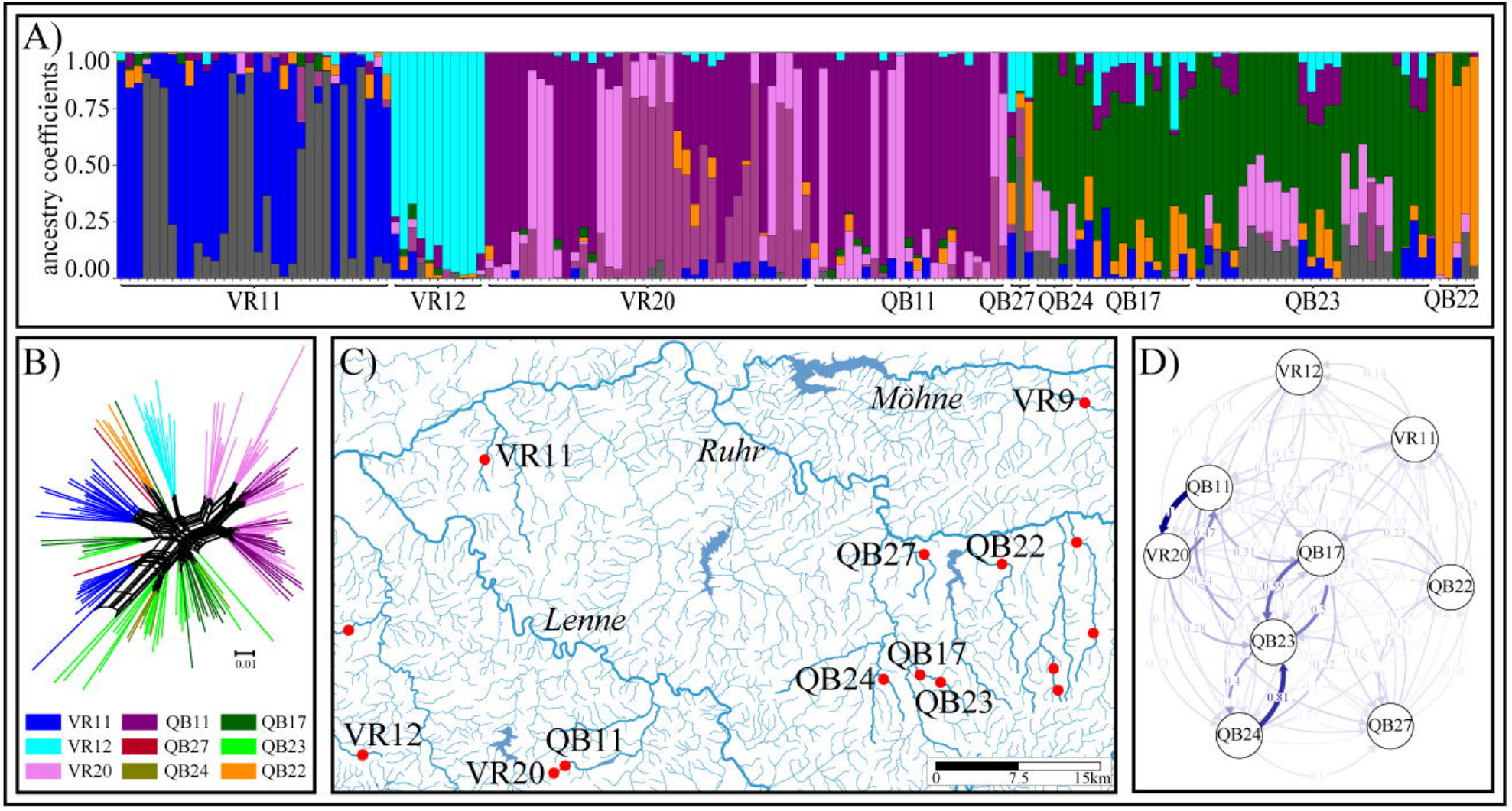
A)
ancestry coefficients
1.00
0.75
0.50
0.25
0.00
VR11
VR12
VR20
QB11
QB27
QB24
QB17
QB23
QB22
B)
0.01
VR11
VR12
VR20
QB11
QB27
QB24
QB17
QB23
QB22
C)
Möhne
VR9
VR11
Ruhr
QB27
QB22
Lenne
QB17
QB24
QB23
VR12
QB11
VR20
0
7.5
15km
D)
VR12
VR11
QB11
VR20
QB17
QB22
QB23
QB24
QB27

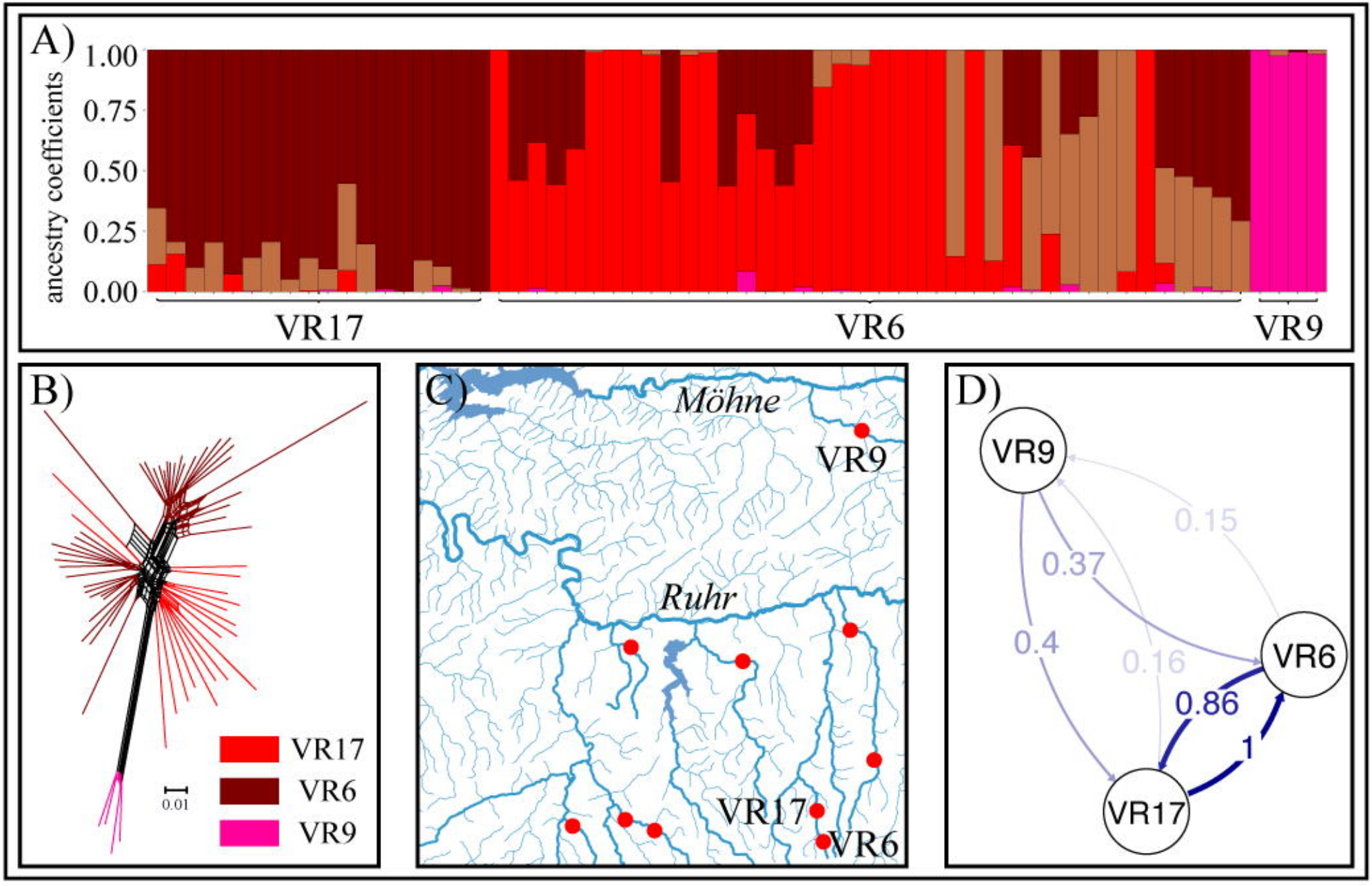
A)
ancestry coefficients
1.00
0.75
0.50
0.25
0.00
VR17
VR6
VR9
B)
VR17
VR6
VR9
0.01
C)
Möhne
Ruhr
VR9
VR17
VR6
D)
VR9
VR6
VR17
0.15
0.37
0.4
0.16
0.86
1

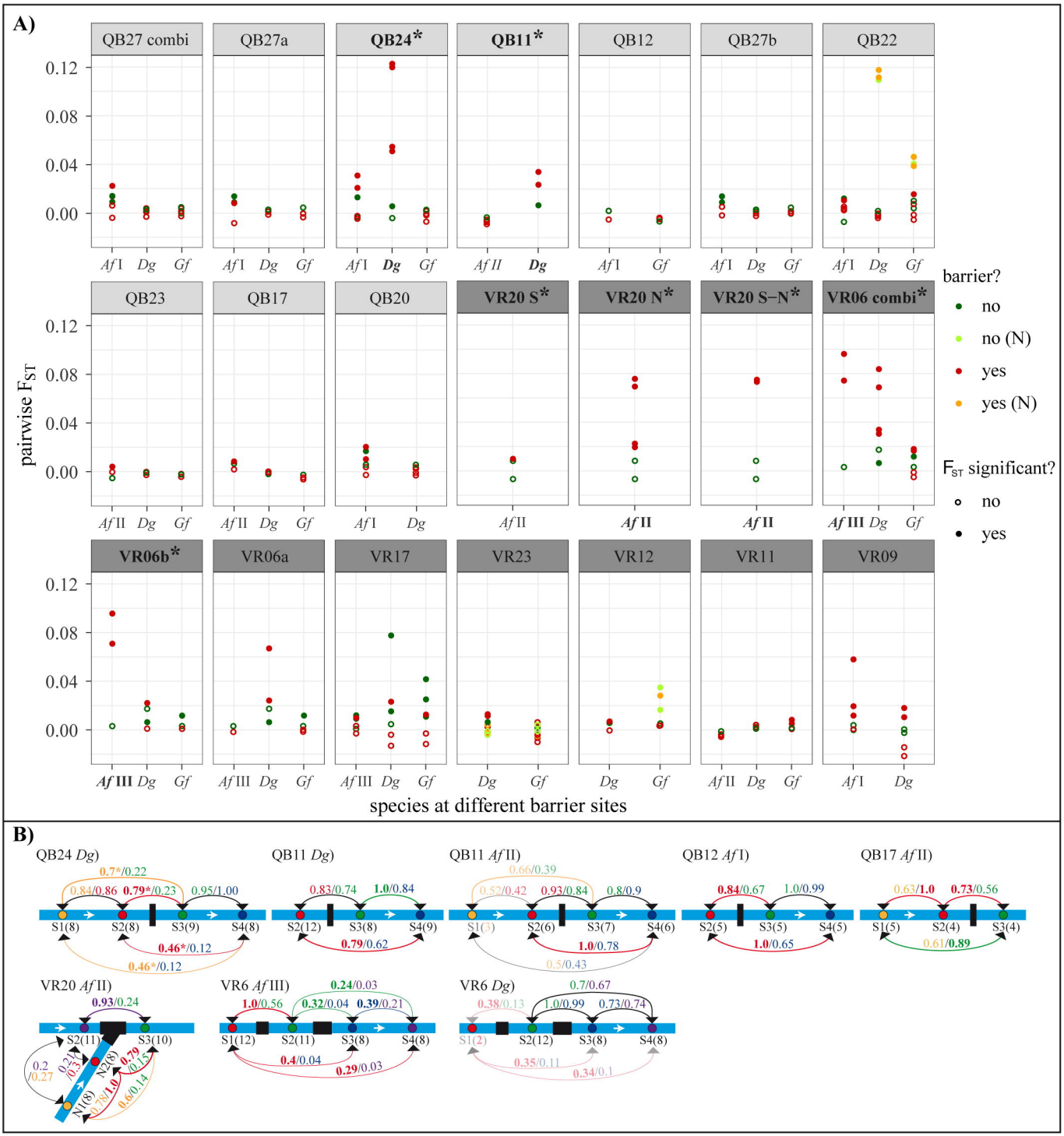
A)
QB27 combi
QB27a
QB24*
QB11*
QB12
QB27b
QB22
QB23
QB17
QB20
VR20 S*
VR20 N*
VR20 S−N*
VR06 combi*
VR06b*
VR06a
VR17
VR23
VR12
VR11
VR09
pairwise $F_{ST}$
species at different barrier sites
barrier?
no
no (N)
yes
yes (N)
$F_{ST}$ significant?
no
yes
B)
QB24 Dg)
QB11 Dg)
QB11 Af II)
QB12 Af I)
QB17 Af II)
VR20 Af II)
VR6 Af III)
VR6 Dg)